

**SYNERGY OF VEGETATION AND SOIL MICROWAVE  
SCATTERING MODEL FOR LEAF AREA INDEX RETRIEVAL USING  
C - BAND SENTINEL - 1A SATELLITE DATA**

---

**5.1 INTRODUCTION**

The biophysical parameters of crops play an important role for balancing the energy fluxes between land/ atmosphere interfaces. Leaf surfaces are the main part of crops responsible for exchanges of mass and energy, regulate processes like evapotranspiration, canopy interception, photosynthesis and can be assessed using Leaf Area Index (LAI). LAI can be estimated in the field both by direct and indirect methods. Direct methods involve destructive sampling, while indirect methods are based on canopy transmittance etc. Since, the direct methods are time consuming and labour intensive, hence some new methods based on remote sensing techniques have been developed using optical and IR regions of electromagnetic spectrums. These methods can be broadly divided into the following categories (1) empirical relationships (for e.g. between LAI and vegetation indices; (2) inversion of models based on canopy reflectance; and (3) fusion of one or more inversion methods.

All the above methods are available in the technical literature domain and their performances vary due to the heterogeneity, sensor resolution, penetration power, atmospheric noises, and weather problems etc. Therefore, there is always a need of improved methods for LAI estimation. The vegetation parameters retrieval using microwave scattering model are mainly affected by the heterogeneous distribution of land targets, which leads to

reduction of the robustness of inversion results for the physical and biophysical processes (Jarlan et al. 2008; Sabater et al 2008; Ferrazzoli et al. 1997; Atzberger, 2004; Ulaby et al. 1986).

In order to retrieve crop growth variables from space platform using microwave remote sensing techniques (i.e. SAR information), various physical, empirical, semi-empirical algorithms have been developed. The semi - empirical water cloud model (WCM) was proposed by Attema and Ulaby (Attema and Ulaby, 1978). The WCM quantifies the relationship between backscattering coefficient ( $\sigma^0$  (dB)) and crop growth parameters by adding the soil information (soil moisture). In the previous studies, the total  $\sigma^0$  (dB) echoes in WCM are mainly composed due to volume scattering from the vegetation. For the sparse vegetation condition, the bare soil scattering responses are not included in WCM. However, these kinds of uncertainties and incompleteness factors in WCM may restrict the retrieval accuracy of biophysical parameters (Inoue et al. 2014). Oh et al. (2004) proposed the direct soil scattering algorithm for the bare soil to measure the correct amount of soil backscatter echoes using soil roughness and soil moisture parameters at different polarizations mode. Therefore, the vegetation coverage and influences of bare soil on the total  $\sigma^0$  (dB) were introduced by the synergy of two modified microwave scattering algorithms for more accurate monitoring of crop growth variables.

In the thesis work, the main focus was to investigate the capability of the C-band Sentinel - 1A SAR data to retrieve LAI using synergy of two modified vegetation (MWCM) and direct soil scattering models (MSSM). The modification of both scattering models was done by introducing a scale invariant vegetation fraction cover ( $f_{veg}$ ) parameter, computed from Landsat-8 satellite data. The non-linear least square optimization techniques were used for parameterization of developed model. Finally, a look-up table (LUT) inversion algorithm was performed for the retrieval of LAI values in the proposed study areas. Furthermore, the

well-established PROBA - V and MODIS - LAI satellite data were also used to evaluate the robustness of retrieved LAI values through the modified model.

## 5.2 STUDY AREA AND DATA COLLECTION

A part of Varanasi district in India was chosen for the retrieval of LAI using proposed methodology. The study area having center latitude  $25^{\circ} 17' 51''$  N and longitude  $82^{\circ} 56' 36''$  E, covering a total area of  $192 \text{ km}^2$ , is shown in Figure 5.1. The sampling fields were covered with Rabi season (cultivated from November to March) crops (mostly wheat and barley). The average field size of campaign sites were 15 m to 30 m for wheat and barley crops. The moist subtropical climate with seasonal variations between winter and summer monsoon and flat topography exists in the study region with the slope variation of 0%–3%.

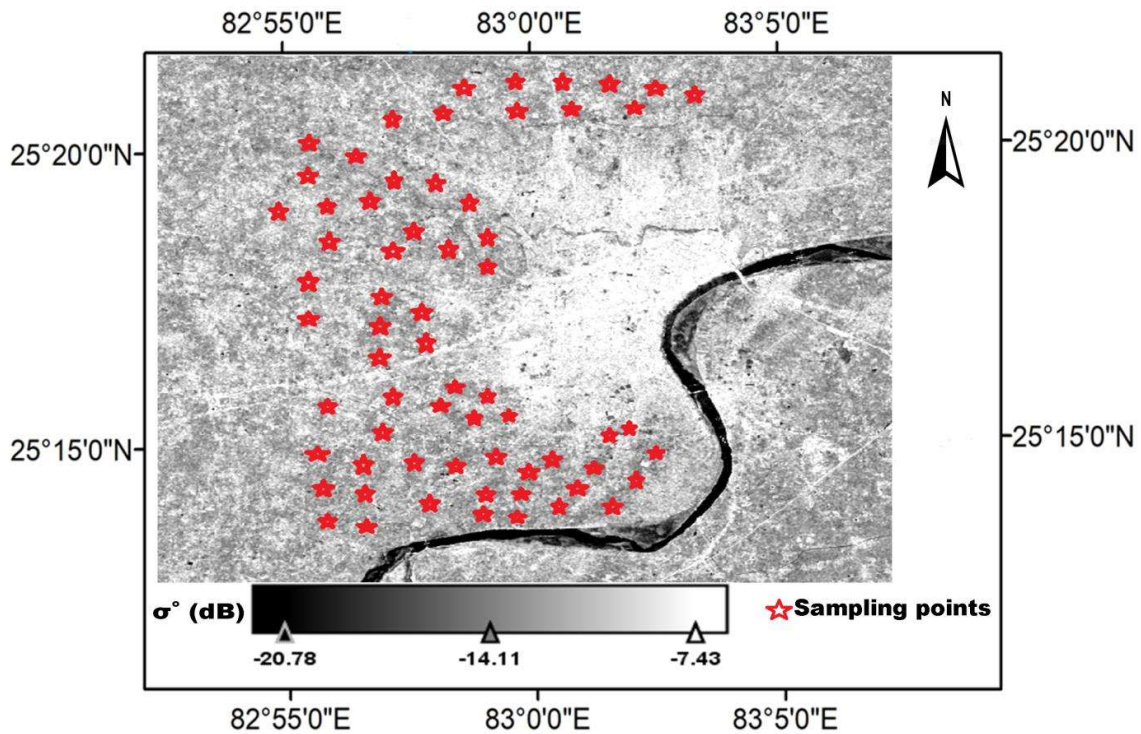


**Figure 5.1.** Geo-location of study region with different sampling points (March 08, 2018 at VV channel)

### 5.2.1 In –situ measurements

The field experiments were performed during February 05, March 08 and March 27, 2018 in agricultural fields (wheat and barley). In each sampling field, every point, representative of an area of 10 m × 10 m, was chosen to measure volumetric soil moisture contents ( $M_v$ ), roughness parameters, and LAI. The average of four measurements was computed as the final value of LAI,  $M_v$  and roughness parameters at spatial pixel size of 20 m × 20 m. The LAI measurements were made at each sampling sites using the LAI - 2200C plant canopy analyzer (LI - COR, Inc.). The  $M_v$  values were taken from a depth of 0 - 5.0 cm at each ground locations using Hydra Probe time domain reflectometry sensor. Whereas, the roughness parameters including surface r.m.s. height (s) were computed using a one meter long soil profilometer. The surface roughness profile was drawn on the board by placing the spokes using ink marker. Finally, the profile photograph of surface roughness was digitized to compute the roughness values. At last, the auto-correlation function techniques were used to compute the correlation length (l).

### 5.2.2 Satellite data

In the present study, the Sentinel - 1A (C - band) synthetic aperture radar (SAR) and Landsat-8 satellite data were used to exploit the capability of synergetic model. The primary image preprocessing of SAR data was completed in SNAP tools followed by geometric correction and radiometric calibration. The orbit file correction and thermal noise removal were performed with Sentinel - 1A GRD data in SNAP tool. An enhanced Lee filter was used to reduce the speckle noise. SAR intensity image was converted into dB from the linear scale (Kumar et al. 2018). The Landsat-8 optical images were used for this study to compute  $f_{veg}$  as a vegetation fraction parameter in MWCM. At last, the images were co-registered according to Sentinel-1A.

**Table 5.1.** Satellite data specifications

<b>A) SAR (Synthetic Aperture Radar) data.</b>						
<b>Satellite</b>	<b>Acquisition</b>	<b>Polarization</b>	<b>Resolution</b> (m × m)	<b>Level</b>		
<b>Sentinel - 1A</b>	05/02/2018	VV/VH	5 × 20	L1		
	08/03/2018	VV/VH	5 × 20	L1		
	25/03/2018	VV/VH	5 × 20	L1		
<b>B) Optical data</b>						
<b>Satellite</b>	<b>Acquisition</b>	<b>bands</b>	<b>Resolution</b> (m)	<b>Swath</b> (km )	<b>Level</b>	
<b>Landsat - 8 (OLI)</b>	05/02/2018	11	30	185	L1	
	07/03/2018	11	30	185	L1	
	27/03/2018	11	30	185	L1	

### 5.3. METHODOLOGY

#### 5.3.1. Modified water cloud model (MWCM)

The WCM, initially proposed by Attema and Ulaby, 1978, considers the vegetation canopy and vegetation layer as a homogeneous anisotropic scattering in order to ignore the multiple scattering effects between vegetation and soil. Thus, the total backscattering ( $\sigma_T^0$ ) is formulated as:

$$\sigma_T^0 = \sigma_{veg}^0 + \tau^2 \sigma_{soil}^0 \quad (5.1)$$

$$\sigma_{veg}^0 = AV_1^E \cos \theta \left[ 1 - e^{-\frac{2BV_2}{\cos \theta}} \right] \quad (5.2)$$

$$\tau^2 = e^{-\frac{2BV_2}{\cos \theta}} \quad (5.3)$$

where  $\sigma_{veg}^0$ ,  $\sigma_{soil}^0$  and  $\tau^2$  represent the backscattering due to vegetation, soil and two-way attenuation coefficient through the canopy, respectively.

Further, the WCM can be simplified by using Taylor series expansion

$$\tau^2 = e^{-\frac{2BV_2}{\cos\theta}} = 1 - \frac{2BV_2}{\cos\theta} + \frac{4B^2V_2^2}{\cos^2\theta} - \dots \quad (5.4)$$

Thus, only first two terms of expanded series are inserted in Equation (5.2)

$$\tau^2 = 1 - \frac{2BV_2}{\cos\theta} \quad (5.5)$$

$$\sigma_{veg}^0 = AV_1^E \cos\theta \left[ \frac{2BV_2}{\cos\theta} \right] \quad (5.6)$$

For vegetation descriptor  $V_1 = V_2 = V$ , the Equation 5.6 can be written as:

$$\sigma_{veg}^0 = f_{veg}AV^E \cos\theta \left[ \frac{2BV}{\cos\theta} \right] \quad (5.7)$$

$$\sigma_{veg}^0 = f_{veg}aV^{E+1} \quad (5.8)$$

$$\sigma_T^0 = f_{veg}aV^{E+1} + (1 + bV)\sigma_{soil}^0 \quad (5.9)$$

where  $a = AB$  and  $b = \frac{-2B}{\cos\theta}$  are the model parameters of modified WCM. Whereas  $f_{veg}$  is the scale invariant model of vegetation fraction cover, which can be expressed as:

$$f_{veg} = \frac{NDVI - NDVI_{min}}{NDVI_{max} - NDVI_{min} + \left( \frac{\rho_{NIR}^V + \rho_R^V}{\rho_{NIR}^S + \rho_R^S} - 1 \right) (NDVI_{max} - NDVI)} \quad (5.10)$$

where  $NDVI_{min}$  and  $NDVI_{max}$  are the minimum and maximum normalized difference vegetation index (NDVI) values of vegetation coverage.  $\rho_{NIR}^V$  and  $\rho_R^V$  are the surface reflectance due to vegetation coverage in NIR and RED regions, respectively. While  $\rho_{NIR}^S$  and  $\rho_R^S$  are due to the soil reflectance in NIR and RED regions, respectively, which were computed using Landsat-8 satellite image (Zhang et al. 2006).

### 5.3.2. Modified soil scattering model (MSSM)

The modified soil scattering model (MSSM) is the modified version of Oh model (Oh, 2004). The modification was performed by inserting the scale invariant vegetation fraction ( $1 - f_{veg}$ ) in the model. The Oh model for the soil scattering can be defined as:

$$\frac{\sigma_{VH}^0}{\sigma_{VV}^0} = 0.1 \left( \frac{s}{l} + \sin 1.3\theta \right)^{1.2} \{1 - e^{-0.9(ks)^{0.8}}\} \quad (5.11)$$

After adding the modification factor for soil weighted ( $1 - f_{veg}$ ), the soil backscattering model can be expressed as:

For VV polarization,

$$\sigma_{VV}^0 = \frac{(1-f_{veg})0.11M_V^{0.7}(\cos\theta)^{2.2}[1-e^{-0.32(ks)^{1.8}}]}{0.1\left(\frac{s}{l}+\sin 1.3\theta\right)^{1.2}\{1-e^{-0.9(ks)^{0.8}}\}} \quad (5.12)$$

and for VH polarization

$$\sigma_{VH}^0 = (1 - f_{veg})0.11M_V^{0.7}(\cos\theta)^{2.2}[1 - e^{-0.32(ks)^{1.8}}] \quad (5.13)$$

where  $k = \frac{2\pi}{\lambda}$ ,  $\lambda$  is wavelength, and  $\theta$  is incidence angle.

### 5.3.3. Synergetic form of total backscattering model at VV and VH polarization

The synergistic form of total backscattering for both VV and VH polarizations are provided through Equations 5.14 - 5.17.

For VV polarization

$$\sigma_T^0 = f_{veg}aV^{E+1} + (bV + 1)\sigma_{soil}^{VV} \quad (5.14)$$

$$\sigma_{VV}^T = f_{veg}aV^{E+1} + (bV + 1) \times \left[ \frac{(1-f_{veg})0.11M_V^{0.7}(\cos\theta)^{2.2}[1-e^{-0.32(ks)^{1.8}}]}{0.1\left(\frac{s}{l}+\sin 1.3\theta\right)^{1.2}\{1-e^{-0.9(ks)^{0.8}}\}} \right] \quad (5.15)$$

For VH polarization

$$\sigma_T^0 = f_{veg}aV^{E+1} + (bV + 1)\sigma_{soil}^{VH} \quad (5.16)$$

$$\sigma_{VH}^T = f_{veg} a V^{E+1} + (bV + 1) \times \left[ (1 - f_{veg}) 0.11 M_V^{0.7} (\cos \theta)^{2.2} \left[ 1 - e^{[-0.32(ks)^{1.8}]} \right] \right] \quad (5.17)$$

### 5.3.4. Computation of global LAI data

The PROBA - V and MODIS satellite provide the global LAI products from the space platform which can be effective to compare their LAI data with simulated LAI values from developed algorithm (Fang et al. 2019). The computation technique of LAI can be expressed as:

$$\text{PROBA - V (LAI)} = \text{SF}^P \cdot \text{DN} + \text{Offset} \quad (5.18)$$

$$\text{MODIS (LAI)} = \text{SF}^M \cdot \text{DN} + \text{Offset} \quad (5.19)$$

where DN = Digital number (or pixel value)

$$\text{SF}^P = \text{Scaling factor (PROBA -V)} = \frac{1}{30}$$

$$\text{SF}^M = \text{Scaling factor (MODIS)} = \frac{1}{10}$$

### 5.3.5. Parameterization and inversion of modified synergetic algorithms

Total 195 ground measurements of LAI,  $M_v$  and  $s$  were taken and divided into calibration (two-thirds of the total, i.e., 130) and validation (one - third of the total, i.e., 65) data sets. The model parameters namely  $a$  and  $b$  were determined by the minimization of cost function (C|g) between the observed and modelled backscattering coefficient using nonlinear least square optimization algorithm (Moran et al., 1998).

$$\text{C|g} = \text{Minimize} \left\| \sum_{i=1}^n (\sigma_{ob_i}^0 - \sigma_{mod_i}^0)^2 \right\| \quad (5.20)$$

where  $\sigma_{ob}^0$  and  $\sigma_{mod}^0 = f(\text{LAI}, M_v, s, l)$  are the computed backscattering coefficients derived from the Sentinel - 1A and modelled backscattering coefficients derived by modified algorithm, respectively using Equations 5.14 and 5.16 at VV and VH polarizations, respectively.

For optimal condition of MWCM model, the following constraints were used for the computation of model parameters, which can be expressed as:

$$\nabla g = 2D \left( \sum_{i=1}^n (\sigma_{ob_i}^0 - \sigma_{mod_i}^0)^2 \right)^T \left( \sum_{i=1}^n (\sigma_{ob_i}^0 - \sigma_{mod_i}^0)^2 \right) = 0 \quad (5.21)$$

where,  $\nabla g$  the Derivative matrix (Jacobian) of differentiable function  $(\sigma_{ob_i}^0 - \sigma_{mod_i}^0)^2$  and The term  $D$  in Equation 5.21 is referred as the derivative of Jacobian matrix which depends on the multi-variate parameters (LAI, and soil parameters). Therefore, the optimized model parameters are shown in Table 5.2.

**Table 5.2** Optimized model parameters

Polarizations	<b>a</b>	<b>E</b>	<b>b</b>
VV	0.418	0.803	0.981
VH	0.063	0.176	0.492

During the inversion process of the developed synergetic model, the LUT algorithm was established to retrieve the LAI values based on Sentinel – 1A images and ground measurements. The simulated  $\sigma^0$  (dB) in the forward modeling were generated for a defined range of LAI (0 - 6 m<sup>2</sup>/m<sup>2</sup>). Afterward, the mean square error (MSE) was computed between Sentinel-1A and modeled  $\sigma^0$  (dB) for each validation points and their corresponding LAI values generated when the MSE reaches the minimum value. The MSE is expressed as:

$$MSE = \frac{1}{N} (\sigma_{Sentinel-1A}^0 - \sigma_{mod}^0)^2 \quad (5.22)$$

where N is number of data sets and  $\sigma_{mod}^0 = f(\text{LAI}, M_v, s, l)$ .

## 5.4. RESULTS AND DISCUSSION

### 5.4.1. Assessment of in-situ measurements and Sentinel-1A $\sigma^0$ (VV/VH) data

Figure 5.2 showed the correlation matrix plot between three major observations, namely Sentinel-1A  $\sigma_{VV}^0, \sigma_{VH}^0$  and ground measured LAI. The  $\sigma_{VV}^0$  was found highly correlated with the LAI ( $r = 0.74$ ) than the  $\sigma_{VH}^0$  ( $r = 0.39$ ), which indicates that the VV polarization is most sensitive to the vegetation cover than the cross polarization. Moreover, the  $M_v$  showed better correlation at VV ( $r = 0.60$ ) than VH ( $r = 0.43$ ) polarization. The attenuation of VV signal occurs due to erectophile plant geometry (wheat and barley). Hence, there are less chances of VV signal penetration into cereal crops, which is in agreement with the previous study (Prevot et al. 1993).

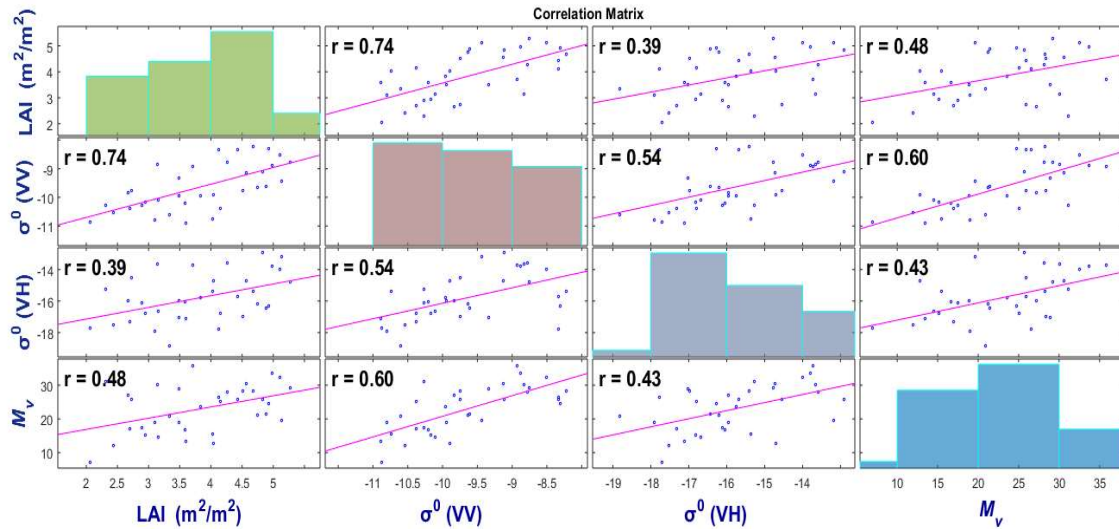
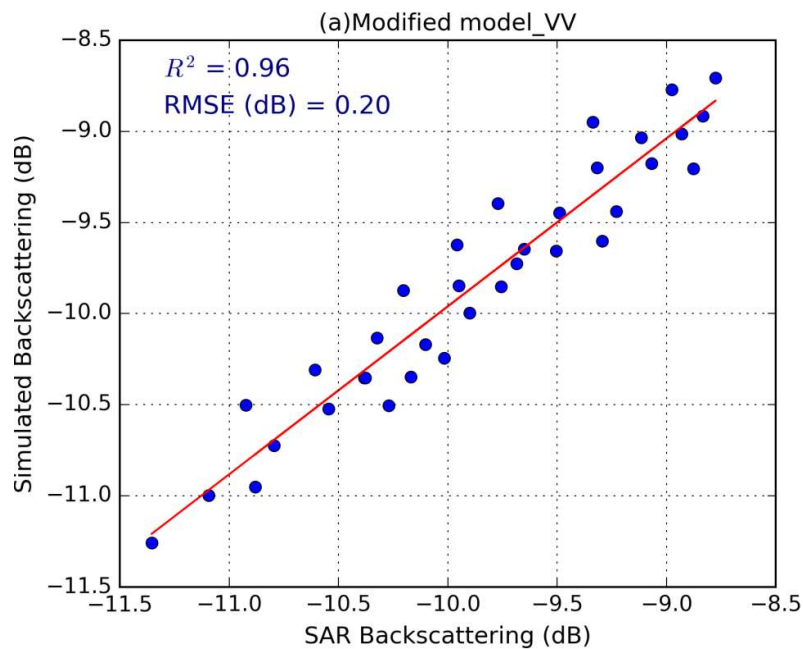


**Figure 5.2** Correlation matrix for in-situ measurements

### 5.4.2. Sensitivity of modified algorithm in forward modeling simulation

Before applying the modified synergetic algorithm of vegetation and soil for the retrieval of LAI, the  $f_{veg}$  was resampled to the Sentinel-1A pixel size for the same geo-location of sampling fields. In order to verify the strength of modified model, two-thirds of the pooled data were randomly chosen for the calibration of developed algorithm and its

model parameters computation. Whereas, the rest data was used for validation of algorithm at inversion process. Figure 5.3 (a, b) provides the scatterplots between the simulated backscattering coefficient and Sentinel-1A backscattering coefficient at VV and VH polarizations. The performance indices indicated a higher  $R^2 = 0.96$  and low RMSE = 0.20 (dB) as compared to VH polarization ( $R^2 = 0.76$  and RMSE = 0.96 (dB)). Thus, the VV polarization may reveal higher sensitivity of modeled  $\sigma^0$  values with the computed Sentinel - 1A  $\sigma^0$  than at VH polarization.



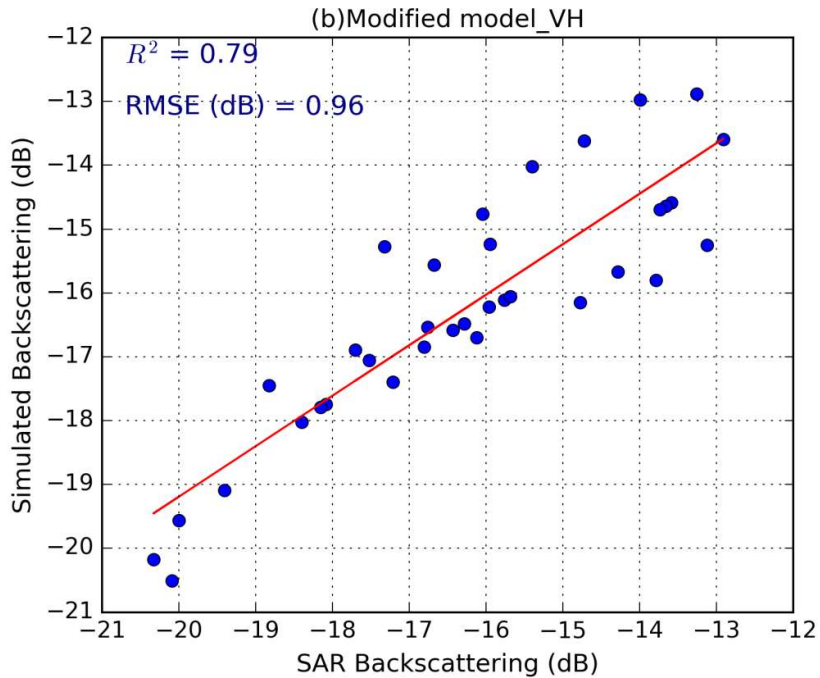
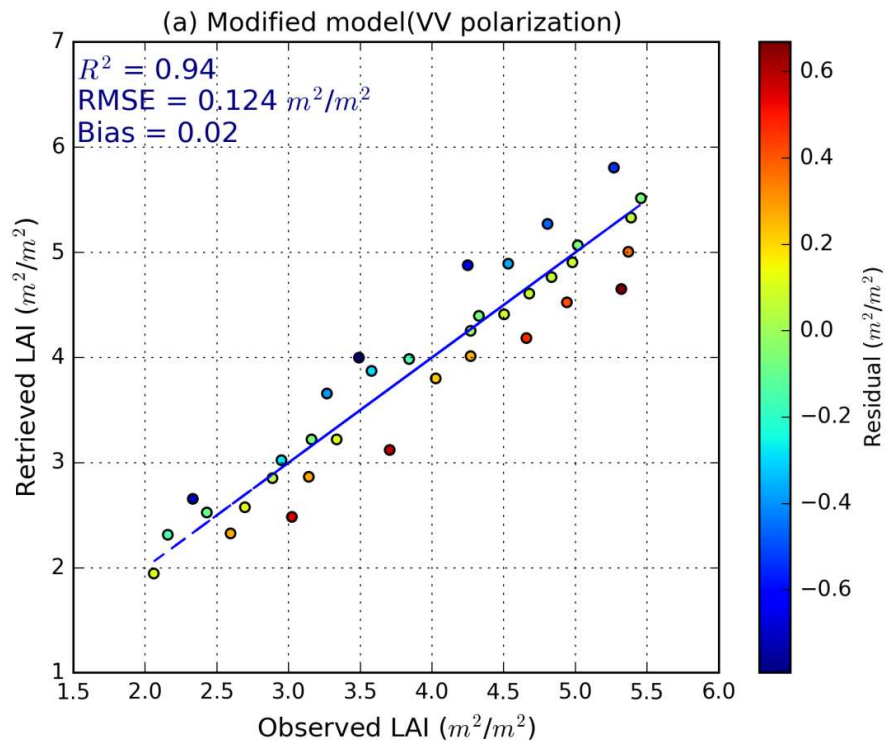


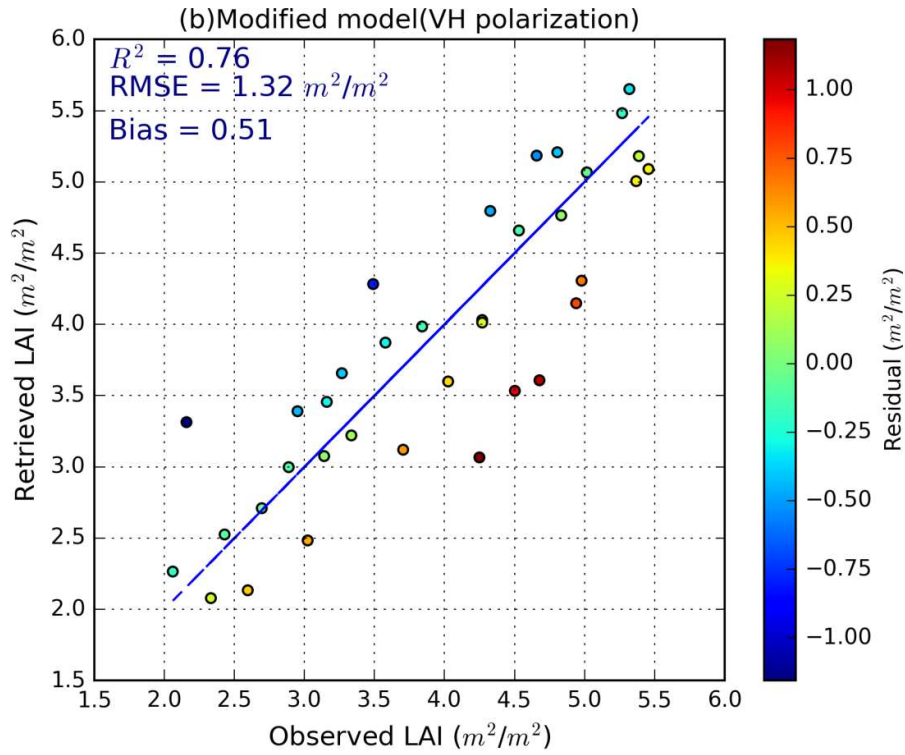
**Figure 5.3** Comparison between SAR and simulated backscattering coefficient at the (a) VV and (b) VH polarization for forward modeling

#### 5.4.3. Retrieval of LAI values (inverse modeling) using LUT inversion approach

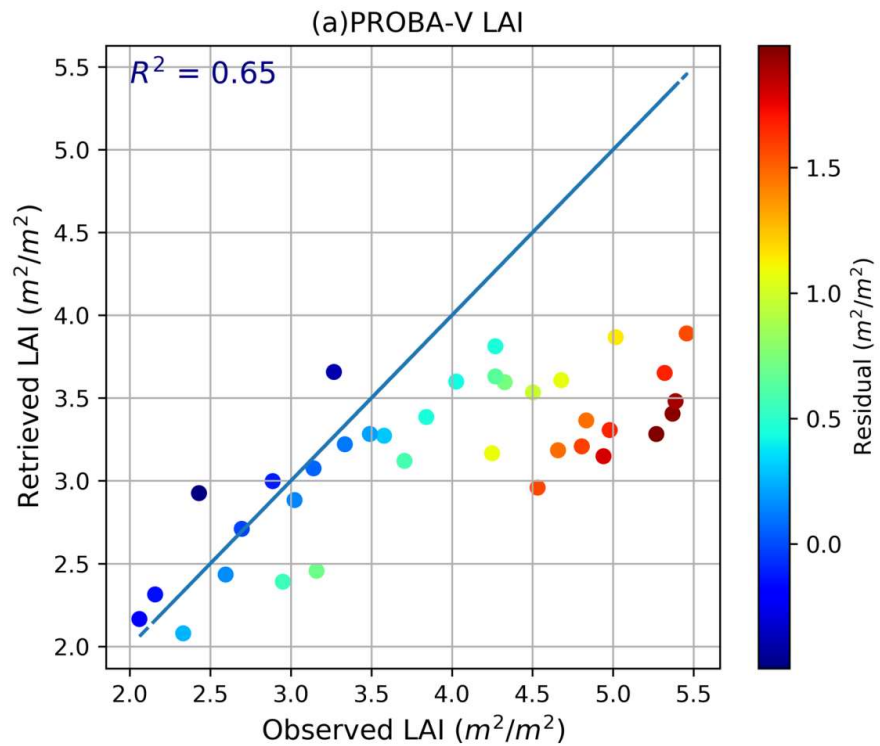
The LAI retrieval was performed, from Equations 5.14 and 5.16 at VV and VH polarization, using nonlinear least square optimization algorithms followed by LUT inversion techniques. In order to evaluate the reliability of proposed modified algorithm, the correlation plots were drawn between modeled LAI and in situ LAI values. Figure 5.4 (a,b) showed the scatter plot between retrieved LAI through modified synergetic algorithm and observed data at VV and VH polarizations, respectively. The statistical indices results showed higher sensitivity of the retrieved LAI with in-situ LAI at VV polarization than at VH polarization. The higher  $R^2 = 0.94$  and lower  $RMSE = 0.124 \text{ m}^2/\text{m}^2$  were found at VV polarization. Whereas, VH polarization showed comparatively lower sensitivity ( $R^2 = 0.76$  and  $RMSE = 1.32 \text{ m}^2/\text{m}^2$ ) with the observed data. The bias value was found to be 0.02 at VV and 0.51 at VH polarizations. Thus, the developed synergetic algorithm at VV polarization showed the

promising retrieval results and comparatively had less influence of saturation effect during inversion of model than at VH polarization. The developed algorithm showed a saturation effect during the inversion process of the LAI values between 5 and 6  $m^2/m^2$ , which could be ascribed to the headings of the wheat and barley crops. Perhaps, the Sentinel - 1 A, C-band, is not able to distinguish the heading and leaves of the wheat and barley crops which may provide some insight of retrieval accuracy through developed algorithm (Hosseini et al. 2015). Furthermore, Figure 5 (a,b) showed the comparative analysis of LAI values for well-established operational global satellite like PROBA - V and MODIS products. The retrieved LAI values from by the synergetic algorithm (microwave response) were found highly accurate than the optical sensors.





**Figure 5.4** Comparison between in-situ and retrieved LAI by the modified model at (a) VV and (b) VH polarization



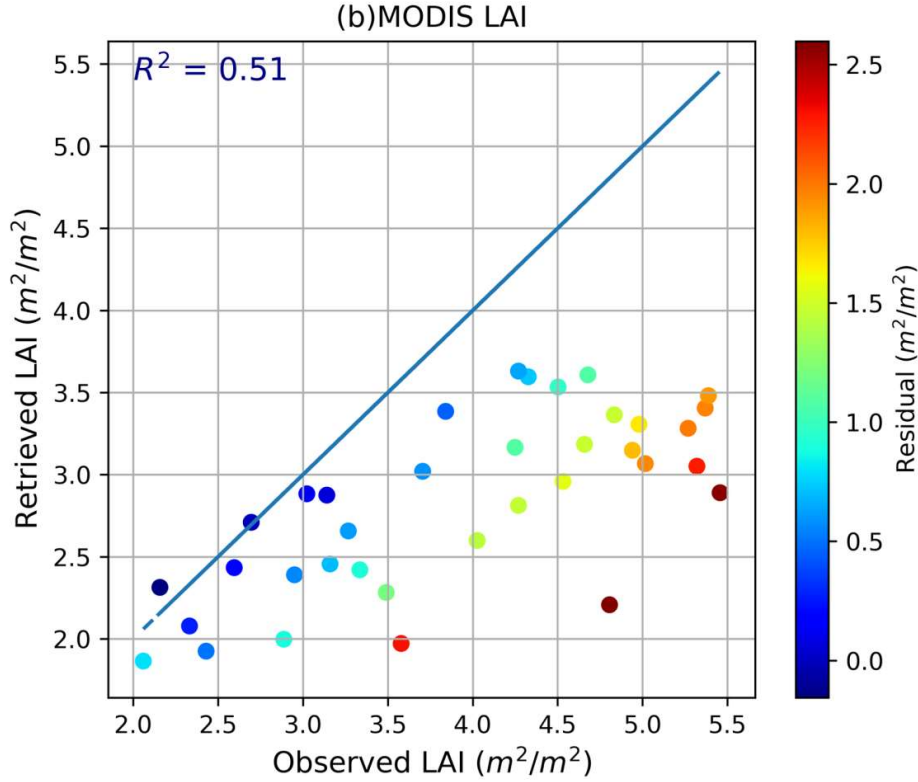


**Figure 5.5** Comparison between in-situ and retrieved LAI by the (a) PROBA-V (b) MODIS global satellite product

#### 5.4.4. Sensitivity of $f_{veg}$ in the synergetic scattering algorithm

In agriculture areas, the satellite sensed spectral pixels were found mixed with crops and bare soil with some area fraction  $f_{veg}$  for crops and  $(1 - f_{veg})$  for the bare soil. Here, pixels were considered to be approximately linear combination of all vegetation and soil components. However, for mixed pixels, the crops reflectance was more than soil in *NIR* and *RED* region. Therefore, the sum of  $\rho_{NIR}^V + \rho_R^V$  was much greater than  $\rho_{NIR}^S + \rho_R^S$  in Equation 5.10. Consequently, it led to contribution of vegetation scattering dominancy in synergetic algorithm where crops reflectance or the effect of vegetation parameters was dominating than the soil reflectance. At some crop phenological stages, the vegetation and soil reflectances

were found nearly equal i.e.  $\rho_{NIR}^V + \rho_R^V \sim \rho_{NIR}^S + \rho_R^S$ , the Equation 5.10 turns to traditional vegetation fraction developed by Gutman and Ignatov, 1998.

#### 5.4.5. Comparison of LAI retrieval algorithms using Taylor plot

Figure 5.6 showed Taylor plot for comparative performance evaluation of the retrieval of LAI values through proposed algorithm and well established global satellite LAI products like MODIS and PROBA - V. Therefore, the Taylor plot indicated higher correlation, low bias and very less standard deviation at VV polarization (A). Whereas, the others like modified algorithm at VH polarization (B), PROBA - V (C) and MODIS (D) indicated lower performance with the observed data. Therefore, this modified algorithm could approximate the higher retrieval LAI values for cereal crops (wheat and barley) than the others modified existing models.

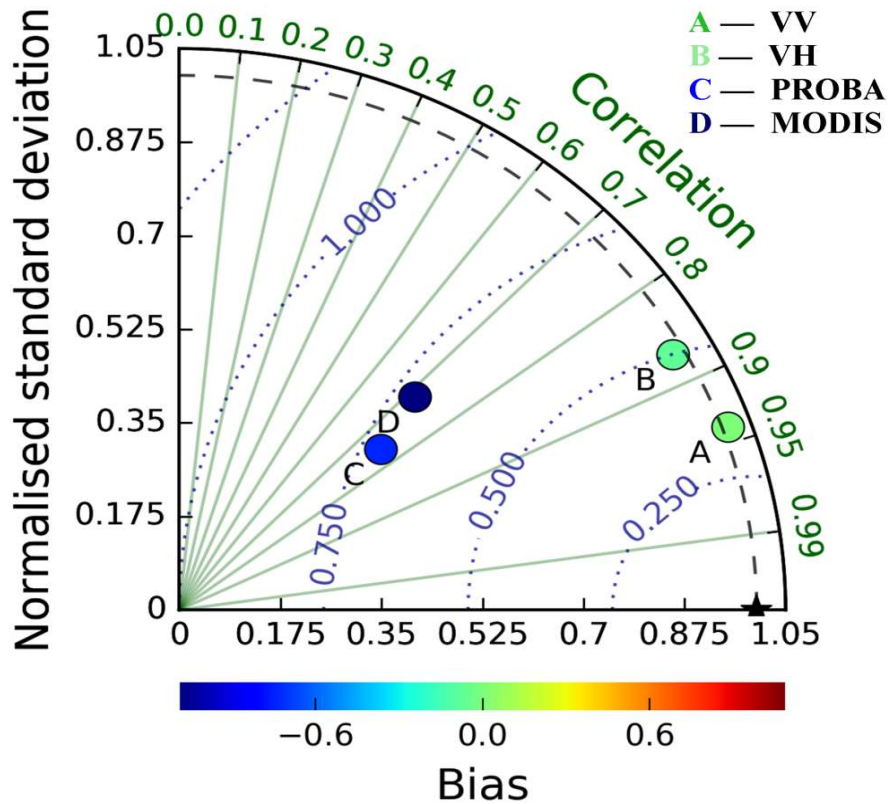


Figure 5.6 Comparative analysis of retrieved LAI using Taylor plot

## 5.5. CONCLUSION

In this chapter, the modified synergetic backscattering model of vegetation (i.e. MWCM) and direct scattering model of soil (i.e. MSSM) were used for the retrieval of LAI over crop using C - band (5.84 GHz) Sentinel - 1A images and scale invariant  $f_{veg}$  parameter computed from Landsat -8 data. The inverse modeling results indicated a high potential of the proposed modified synergetic algorithms to retrieve LAI more accurately at finer spatio-temporal resolutions. In the forward modeling, the simulated  $\sigma^0(dB)$  in VV channel of the MWCM was found better than that of VH polarization. However, the retrieval performance of LAI values for inverse modeling scheme indicated higher relationship with in-situ measurements at VV polarization ( $R^2 = 0.94$  and  $RMSE = 0.124 m^2/m^2$ ) than that of well established on-board PROBA - V and MODIS LAI products. Therefore, the synergy of MWCM and MSSM model provides a new tool for the inversion of biophysical parameters by coupling the recent advances of SAR and optical satellite data. Moreover, due to the limitation and unavailability of fine resolution LAI satellite data product, this modified algorithm could be used as an alternative approach to simulate LAI over agricultural fields for ongoing and future satellites missions.